ALLEVIATION OF TILTROTOR WING-ROOT VIBRATORY LOADS THROUGH CYCLIC CONTROL APPROACH

M. Molica Colella, G. Bernardini and M. Gennaretti
University Roma Tre, Dept. of Mechanical and Industrial Engineering,
Via della Vasca Navale 79 - 00146 Rome, Italy

Abstract

This paper examines the application of control systems for the alleviation of the vibratory loads transmitted to the airframe by the wing-proprotor system of a tiltrotor in uniform, rectilinear flight. The control action is based on the introduction of higher harmonics in the proprotor blade cyclic pitch motion, and in the cyclic actuation of controllable-stiffness devices located at the roots of the blades. Control laws are obtained through an optimal control methodology that yields the best compromise between control effectiveness and control effort. The numerical investigation concerns the analysis of the performance of the control techniques applied, examining a XV-15 tiltrotor model in airplane mode configuration.

1. INTRODUCTION

This work deals with the application of optimal control techniques to alleviate vibratory loads arising on the wing-proprotor system of a tiltrotor. Indeed, hub loads generated by the proprotor, along with the aerodynamic interactions between the wing and the wake of the blades produce vibratory loads on the wing that, at the root, are transmitted to the fuselage. In turn, they produce acoustic disturbance inside the cabin that may cause unacceptable ride discomfort, and have also a significant impact on the fatigue-life of the structure (and hence on maintenance costs), thereby being a critical issue for tiltrotor designers. This explains why the suppression/alleviation of wing-root vibratory loads is one of the goals that deserves the attention of rotorcraft designers and researchers (see, for instance, the control approaches based on wind-tunnel test data presented in Refs. 1 and 2, respectively for airplane mode and helicopter mode applications).

Here, we examine the reduction of the vibrating wing-root loads both through the introduction of higher harmonics in the actuation of the proprotor cyclic pitch, and by the cyclic actuation of less conventional IBC devices like smart-springs[3] at the blade root, that are able to induce local bending stiffness variations. Specifically, the investigation is aimed at the analysis of the effectiveness of such control techniques. The laws of the actuation of cyclic pitch higher harmonics and smart springs are obtained by an optimal control methodology based on the minimization of a cost function, which includes vibratory loads and control input harmonics, under the constraint of compatibility with equations governing the wing-proprotor aeroelasticity.

As it will be shown in Section 3, the identification of the cyclic control law requires the knowledge of the (sensitivity or gradient) matrix that relates the harmonics of the control inputs to the corresponding vibratory loads. In this work it is obtained numerically through computational predictions of the wing-proprotor aeroelastic behaviour. To this purpose, a wing-proprotor aeroelastic solver developed in the past by the authors[4] has been adapted to include the effects of the control variables, and then applied. It considers an aerodynamic model based on a boundary integral formulation for the velocity potential that is able to take into account the aerodynamic interference between wing and proprotor, with inclusion of the effects of impacts between wake vortices and body surfaces.[5] This formulation is fully three-dimensional, can be applied to complete aircraft/rotorcraft configurations in ar-

bitrary motion, and allows the calculation of both wake distortion (free-wake analysis) and velocity field induced by the wake. In turn, the latter is coupled with a quasi-steady airfoil theory to predict loads forcing blades and wing. The structural dynamics of wing and proprotor blades is described by beam-like models,[6] with inclusion of the wing-proprotor mechanical interaction, that is mainly governed by the influence of wing deformation on the kinematics of the blades and by transmission of proprotor loads to the wing through hub and pylon. This formulation yields a set of coupled, nonlinear, integro-differential equations, governing bending and torsion of wing and proprotor blades. Additional equations are included when a gimballed proprotor is examined. The resulting aeroelastic model for wing-pylon-proprotor system is solved through the application of the Galerkin method for space discretization, followed by a harmonic balance approach for time integration.[7]

2. VIBRATORY LOADS ANALYSIS

In the aeroelastic tool applied for the analysis of tiltrotor vibratory loads the equations governing the structural dynamics are coupled with a quasi-steady aerodynamic model in which the wing-proprotor interaction effects are included through the induced velocity model. Here, the velocity induced by the wake vorticity is obtained by a three-dimensional, unsteady, panel-method tool which is able to capture the effects of the aerodynamic interference between rotor and wing, including the strong rotor-wake/wing interaction. In the following, the aeroelastic solver applied in the control law identification process and validation phase is briefly outlined, along with the aerodynamic model used for the determination of the velocity field induced by the wake.

2.1 The aeroelastic formulation

Beam-like models are applied to describe the structural dynamics of both wing and rotor blades. They are based on the nonlinear bending-torsion equations of motion presented in Ref. 6, that are valid for straight, slender, homogeneous, isotropic, nonuniform, twisted wing/blades. Retaining second order terms after the application of an ordering scheme that drops third-order terms not contributing to damping, and assuming radial displacements as simply geometric consequences of the transverse bending deflections,[8] the final form of the dynamic system is a set of coupled nonlinear integro-partial differential equations having as unknowns the displacements of the elastic axis, along with the cross-section elastic torsion. It is suitable for describing the response of beam-like structures undergoing significant deflections. In the aeroelastic tool for control design, both wing and proprotor aerodynamic loads are simulated through 2D, quasi-steady, aerodynamic models (with wake-inflow corrections, to take into account unsteady and three-dimensional effects due to wake vorticity).

The kinematics of the rotor blades is strongly affected by the motion of the wing section to which the rotor is attached to through the pylon structure. Thus, both aerodynamic and inertial blade forcing terms are significantly dependent on the elastic deformation of the wing. On the other hand, in addition to the aerodynamic loads, wing dynamics is forced by forces and moments transmitted by the proprotor at the wing section where the pylon is located and by the inertial effects due to the pylon mass.

The combination of wing and proprotor aeroelastic models yields a strongly coupled set of equations governing the aeroelasticity of the wing-pylon-proprotor system to be integrated. To this aim, the space discretization of both wing and proprotor blade equations is performed through the Galerkin method, starting from elastic deformations described as a linear combination of suitable linearly independent shape functions that satisfy the geometric homogeneous boundary conditions corresponding to the structure constraints (in this work, the natural modes of a cantilever beam have been applied).[7] The resulting aeroelastic system consists of a set of nonlinear ordinary differential equations of the type

$$\begin{aligned} &\mathbf{M}(t)\,\ddot{\mathbf{q}} + \mathbf{C}(t)\,\dot{\mathbf{q}} + \mathbf{K}(t,\mathbf{k}_u)\,\mathbf{q} = \\ &\mathbf{f}_{str}^{nl}(t,\mathbf{q},\mathbf{k}_u) + \mathbf{f}_{iner}^{\theta}(t,\mathbf{q},\theta) + \mathbf{f}_{aer}(t,\mathbf{q},\theta) \end{aligned} \tag{1}$$

where $\mathbf{q}$ denotes the vector of the Lagrangean coordinates of blade (with inclusion of gimbal degrees of freedom, if present), θ denotes the higher harmonic blade cyclic motion used as a controller, $\mathbf{k}_u$ is the vector of the blade bending

stiffness control variables, whereas $\mathbf{M}, \mathbf{C}$, and $\mathbf{K}$ are time-periodic, mass, damping, and stiffness structural matrices representing the linear structural terms. Nonlinear structural contributions are collected in $\mathbf{f}_{str}^{nl}$, the inertial loads due to higher harmonic blade cyclic motion are collected in $\mathbf{f}_{iner}^{\theta}$, whereas the generalized aerodynamic forces are collected in $\mathbf{f}_{aer}$ (with inclusion of aerodynamic loads transmitted to the wing by the proprotor).

Considering problems concerning tiltrotors in uniform rectilinear motion (during which wing and proprotor blades are subject to steady periodic deformations), the blade passage frequency is the fundamental frequency of wing response, whereas the fundamental frequency of proprotor blade response is the rotor frequency of revolution. Thus, the solution of Eq. (1) and hence the prediction of the vibratory loads is based on a harmonic balance approach. It is a methodology suitable for the analysis of asymptotic solutions of differential equations (as time goes to infinity) forced by periodic terms, as in the present problem. The harmonic balance solution consists of: (i) express LHS and RHS of Eq. (1) in terms of Fourier series; (ii) equate the resulting coefficients; (iii) solve the corresponding algebraic set of equations in terms of the unknown Fourier coefficients of the Lagrangean coordinates of the problem. Note that, because of the presence of nonlinear terms, the harmonic balance solution requires an iterative procedure.

2.1 The three-dimensional, unsteady, aerodynamic formulation

The aerodynamic field of wing-rotor systems is dominated by the interaction effects occurring between rotor blades and wing. Periodic blade passages close to the wing are a first source of oscillations of the pressure field over wing and proprotor blades, but the main source of wing unsteady aerodynamic loads is given by the impact of rotor wake vortices on wing surface. Indeed, the wing located behind the propeller is massively impinged by the wake vorticity released by the rotor blades: this generates local flow and pressure perturbations that, in turn, yield a significant contribution to the vibrating loads. The accurate analysis of problems involving the strong interaction between vortices and bodies is a complex task that requires the application of suited three-dimensional, unsteady aerodynamic solver.

To this aim, here the boundary integral formulation for potential flows introduced in Ref. 5 has been applied. It is a development of the formulation presented in Ref. 9, which overcomes instabilities of the numerical solution arising in case of impingement between wake and body surfaces. This formulation introduces the decomposition of the potential field into an incident field, φ_I, and a scattered field, φ_S. The scattered potential is generated by sources and doublets over the body surfaces and by doublets over portions of the body wakes that are very close to the trailing edges from which they emanated (near wake, $\mathcal{S}_W^N$). The incident potential is generated by doublets over the complementary wake regions that compose the far wakes, $\mathcal{S}_W^F$. These are the wake portions that may come in contact with other body surfaces (note that, in the present analysis, body surface denotes proprotor blades and wing surfaces, while the wake surface includes wakes from both rotor blades and wing). The scattered potential is discontinuous across $\mathcal{S}_W^N$, whereas the incident potential is discontinuous across $\mathcal{S}_W^F$. Hence, as demonstrated in Ref. 5, for $\varphi = \varphi_I + \varphi_S$ the scattered potential is obtained by

$$\varphi_S(\mathbf{x},t) = \int_{\mathcal{S}_B} \left[G\,(\chi - \chi_I) - \varphi_S \frac{\partial G}{\partial n} \right] \mathrm{d}\mathcal{S}(\mathbf{y}) - \int_{\mathcal{S}_W^N} \Delta\varphi_S \frac{\partial G}{\partial n}\,\mathrm{d}\mathcal{S}(\mathbf{y}) \tag{2}$$

where G is the unit source solution and $\Delta\varphi_S$ is the potential jump across the wake surface.[5] In addition, $\chi = \mathbf{v}\cdot\mathbf{n}$ accounts for the impenetrability boundary condition (with $\mathbf{v}$ denoting the body velocity due to rigid and elastic body motion, and $\mathbf{n}$ the surface unit outward normal vector), while $\chi_I = \mathbf{u}_I \cdot \mathbf{n}$, with the velocity induced by the far wake, $\mathbf{u}_I = \nabla\varphi_I$, given by

$$\mathbf{u}_I(\mathbf{x},t) = -\nabla \int_{\mathcal{S}_W^F} \Delta\varphi_S \frac{\partial G}{\partial n}\,\mathrm{d}\mathcal{S}(\mathbf{y}) \tag{3}$$

The incident potential affects the scattered potential by the induced-velocity term, χ_I, and, in turn, the scattered potential affects the incident

potential by its trailing-edge discontinuity that is convected along the wake and yields the intensity of the doublet distribution over the far wake.

Obtaining the zero-th order discrete form of Eq. (3) by using N panels over the far wakes and recalling the vortex-doublet equivalence, the incident velocity field may be evaluated through the following expression

$$\mathbf{u}_I(\mathbf{x},t) \approx -\sum_{n=1}^{N} \Delta\varphi_S(\mathbf{y}_{W_n}^{TE}, t-\theta_n) \int_{\mathcal{C}_n} \nabla_{\mathbf{x}} G \times \mathrm{d}\mathbf{y}$$

where $\mathcal{C}_n$ denotes the contour line of the n-th far wake panel, $\mathbf{y}_{W_n}^{TE}$ is the trailing edge position where the wake material point currently in $\mathbf{y}_{W_n}$ emanated at time $t-\theta_n$, and $\nabla_{\mathbf{x}}$ denotes the operation of gradient with respect to the variable $\mathbf{x}$. This equation represents the velocity field given by the Biot-Savart law applied to the vortices having the shape of the far wake panel contours and intensity $\Delta\varphi_S(\mathbf{y}_{W_n}^{TE}, t-\theta_n)$. The final step of the formulation presented in Ref. 5 consists of introducing in these vortices a finite-thickness core where a regular distribution of the induced velocity is assured, along with a stable and regular solution even in body-vortex impact conditions[5] (it is worth recalling that only the far wake may experience such events). The description of the wake influence through the use of finite-core vortices is a way to include also diffusivity and vortex-stretching effects that, otherwise, would not be taken into account in a potential-flows aerodynamic formulation.

Akin to Eq. (3), Eq. (2) is solved numerically by boundary elements, *i.e.*, by dividing $\mathcal{S}_B$ and $\mathcal{S}_W^N$ into quadrilateral panels, assuming φ_S, χ, χ_I and $\Delta\varphi_S$ to be piecewise constant (zero-th order, boundary element method - BEM), and imposing the equation to be satisfied at the center of each body element (collocation method). Once the potential field is known, the Bernoulli theorem yields the pressure distribution and the integration over the body surface gives the corresponding aerodynamic loads.

3. OPTIMAL CONTROL FOR LOADS ALLEVIATION

Here, the objective is to identify the blade higher harmonic cyclic pitch motion and the cyclic blade root smart spring stiffness variations such that wing-root vibratory hub loads are reduced as much as possible. Following an approach already used in the past by other authors that have faced the problem of helicopter vibration control (see, for instance, Refs. 10, 11, 12, and 13), this is achieved through an optimal methodology that consists of minimizing the following performance index

$$J = \mathbf{z}^{\mathrm{T}}\,\mathbf{W}_z\,\mathbf{z} + \mathbf{u}^{\mathrm{T}}\,\mathbf{W}_u\,\mathbf{u} \tag{4}$$

where $\mathbf{u}$ is the vector collecting the control input amplitudes to be determined (harmonics of higher-harmonic cyclic pitch and blade root bending stiffnesses, in our case), $\mathbf{z}$ is the vector of the quantities to be reduced, while $\mathbf{W}_z$ and $\mathbf{W}_u$ are weighting matrices that are defined so as to get the best compromise between control effectiveness and control effort. Because of the inherently time-periodic nature of the problem, this control approach involves only the harmonics of input and output variables, without concerning the evolution of transients. In the present problem, for a N-bladed proprotor, the output vector consists of the N/rev sine and cosine harmonics of loads to be attenuated, while the control inputs are the sine and cosine higher harmonics of blade pitch, θ and blade root smart spring stiffnesses, $\mathbf{k}_u$, that are effective for control.

Akin to the standard optimal LQR control method (of which the present approach may be interpreted as the natural extension for the application to the control of the steady-periodic behavior of a system governed by a nonlinear, periodic-coefficient differential equation), the minimization of the cost function is obtained under the constraint of satisfying the governing equation of the system controlled. Such constraint is not directly represented by Eq. (1), but rather is given by the following linearized relationship (about a reference input state, $\mathbf{u}_{n-1}$) between control inputs, $\mathbf{u}$, and system response, $\mathbf{z}$,

$$\mathbf{z}_n = \mathbf{z}_{n-1} + \mathbf{T}_{n-1}\,(\mathbf{u}_n - \mathbf{u}_{n-1}) \tag{5}$$

where $\mathbf{T}_{n-1}$ is the (Jacobian) transfer matrix that may be obtained numerically from solutions of Eq. (1). Note that the nonlinear behavior of the rotor aeroelastic response implies that the transfer matrix is not constant, being a function of the reference input state. Then, combining

Eq. (4) with Eq. (5) and minimizing the resulting cost function yields the following optimal control input

$$\mathbf{u}_n = \mathbf{G}_u\,\mathbf{u}_{n-1} - \mathbf{G}_z\,\mathbf{z}_{n-1} \tag{6}$$

where the gain matrices are given by

$$\begin{aligned}\mathbf{G}_u &= \mathbf{D}\,\mathbf{T}_{n-1}^{\mathrm{T}}\,\mathbf{W}_z\mathbf{T}_{n-1}\\ \mathbf{G}_z &= \mathbf{D}\,\mathbf{T}_{n-1}^{\mathrm{T}}\,\mathbf{W}_z\end{aligned}$$

with

$$\mathbf{D} = (\mathbf{T}_{n-1}^{\mathrm{T}}\mathbf{W}_z\mathbf{T}_{n-1} + \mathbf{W}_u)^{-1}$$

Equation (6) has to be used in a recursive way: starting from a given control input and corresponding output, the law of the optimal controller is updated until convergence. This approach yields the gain matrices to be implemented in a closed-loop control process in which, at each n-th control step, measured vibrating hub loads and corresponding control inputs are used as a feedback to update the control law. In this case, the time interval between each control step should be long enough to allow the tiltrotor to reach the steady-periodic state corresponding to the updated control inputs.[10].

A drawback in using this local controller methodology lies in the significant computational cost for the evaluation of the gradient matrix at each step of the control process (note that the evaluation of the gradient matrix requires the determination of the sensitivities of the hub loads harmonics with respect to each flap deflection harmonic considered in the control actuation). In the numerical investigation, here the optimal gain matrices law have been determined through a computationally efficient local controller procedure. It consists of the least square polynomial approximation of outputs as functions of the inputs (based on numerically evaluated open-loop data), from which the elements of the gradient matrix, $\mathbf{T}$, may be derived analytically (a similar procedure has been applied in Ref. 2 for reduction of noise and vibration of the XV-15 rotor). Indeed, this approach significantly increases the numerical efficiency of the local controller, in that allows a search of the optimal control actuation that is as fast as that using a global controller ($i.e.$, considering a constant gradient matrix), and much faster than the local controller one that requires the numerical evaluation of the gradient matrix at each step of the control process.

4. NUMERICAL RESULTS

The control algorithm for the alleviation of vibratory loads at the wing-root has been applied considering the wing-proprotor model examined in Ref. 14. For this configuration, the stability analysis performed by the aeroelastic solver applied here yields results that are in good agreement with those presented in Refs. 14 and 15 (for such a comparison, an aerodynamic model very similar to that described in Ref. 14 has been used).[16] The wing considered has length $L_w = 5.092$m and chord $c = 1.58$m, while the three-bladed gimballed proprotor has radius $R = 3.82$m (see Ref. 14 for further details on the geometrical and structural properties).

The attention has been focused on the airplane mode configuration in level flight, where the main sources of vibratory loads are the interaction aerodynamic effects between wing and proprotor. In this flight condition the free-stream velocity considered is $V = 128.5$m/s and the proprotor angular velocity is $\Omega = 458$RPM (corresponding to advance ratio, $\mu = 0.7$). The wing angle of attack is equal to 3° and the proprotor axis is aligned with the free-stream. The control results that will be presented in the following have been obtained through a control law synthesis obtained from a cost function (see Eq. (4)) that is based on proprotor hub loads as outputs to be reduced. This choice has been motivated by the difficulty in approximating analytically the matrix $\mathbf{T}$ relating control variable harmonics and wing-root vibratory loads (an irregular behaviour is shown by some of these transfer functions, and further research will be addressed to better understand such a problem). The results that will be presented in the following have been obtained limiting the higher harmonic pitch motion to $\pm 0.4^\circ$ and the smart spring cyclic amplitude to the 10% of the baseline stiffness value. In both cases, the control law has been synthesized by using the harmonics from 2/rev to 4/rev.

Figure 1 shows the 3/rev dimensionless loads at the proprotor hub, comparing the uncontrolled ones, with those given by a feedforward control

approach and a feedback control approach, both actuating higher harmonic pitch motion (loads components are given in a frame with y-axis along the wing span and z-axis aligned with the proprotor shaft; they have been obtained by dividing forces by the factor $m\Omega^2R^2$ and the moments by the factor $m\Omega^2R^3$, with $m = 7.64$kg/m). Note that in the feedforward control approach the higher harmonic pitch motion determined in the control law synthesis through matrix $\mathbf{T}$ is directly applied in the aeroelastic tool, while in the feedback control approach matrices $\mathbf{G}_z$ and $\mathbf{G}_u$ are used to determine higher harmonic pitch motion as a function of the measured hub loads. Both approaches significantly reduce the vibratory hub loads, with the feedback one slightly giving better performances. The same comparison is presented in Fig. 2 for the vibratory loads at the wing root (in this case loads components are given in a frame with y-axis along the wing span and vertical z-axis; they have been obtained by dividing forces by the factor $m\Omega^2L_w^2$ and the moments by the factor $m\Omega^2L_w^3$, with distributed mass $m = 32.5$kg/m). Also in this case the vibratory loads are significantly alleviated (although they are not the direct objective of the optimal control), with a poorer performance for the vertical shear and bending moment (again, in the overall the feedback control better alleviate vibrations).

Next, the smart spring control has been applied. The results obtained are presented in Fig. 3 for the hub loads and in Fig. 4 for the wing-root ones. Akin to the higher harmonic pitch control, hub loads are strongly reduced and a good reduction is also obtained for the wing-root loads, although better control performance has been obtained with the higher harmonic pitch actuation.

Finally, Figs. 5 and 6 show the results of the combined control action from higher harmonic pitch motion and smart spring stiffness variation. Comparing these figures with Figs. 1-4 it is possible to observe that using both devices does not change the order of magnitude of the attenuation obtained. Specifically, it gives control performances similar to that achieved by using higher harmonic pitch control only, with a slightly more reduction on the vertical shear but a poorer performance on the out–of–plane bending moment.

5. CONCLUDING REMARKS

A cyclic control approach has been applied to the alleviation of vibratory loads acting on a wing-proprotor system in airplane mode condition. In this configuration the main source of vibrations are the aerodynamic interaction effects between wing and blades. The control synthesis has been based on the numerical evaluation of the sensitivity matrix relating input harmonics to vibratory loads included in the cost function of the optimal control method. Because of the irregular behaviour of some transfer functions involving the wing-root loads, here best control performance has been obtained basing the control approach on the cost function by considering proprotor hub loads. Specifically, a good alleviation of vibratory loads has been achieved using higher harmonic cyclic pitch, higher harmonic smart springs and the combination of them. The application of only higher harmonic cyclic pitch control yields better performances than the application of only smart springs. The use of the combined action of both devices has shown similar performances than those obtained by applying the only higher harmonic cyclic pitch control. In addition, although the control is based on the reduction of proprotor hub loads, it is efficient also in the reduction of wing-root loads. Next research activity is needed in this subject, starting from the analysis of the robustness of the control methodology, and including the investigation about the problems that have been found in determining the control law from an optimal methodology based on the transfer matrix involving directly the vibratory loads at the wing root. Anyway, we expect that the use of combined devices would give better alleviation when the wing–root loads will be included in the cost function.

6. REFERENCES

[1] Nixon, M.W., Kvaternik, R.G., and Settle, T.B., "Tiltrotor Vibration Reduction Through Higher Harmonic Control," American Helicopter Society 53rd Annual Forum, Virginia Beach, Virginia, 1997.

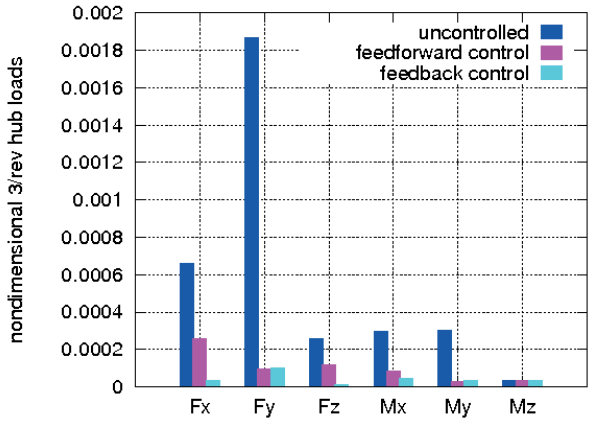

Figure 1. 3/rev proprotor hub loads. Higher harmonic pitch actuation.

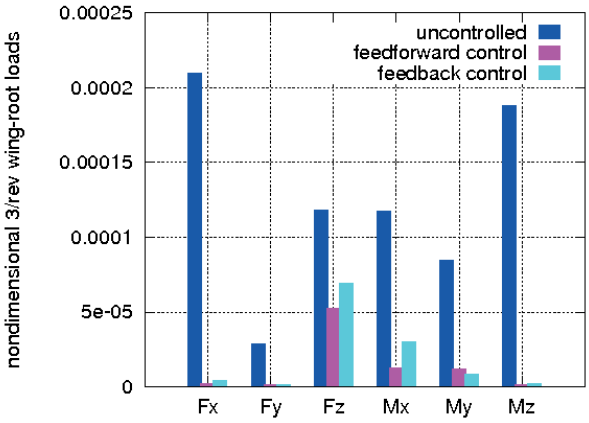

Figure 4. 3/rev wing-root loads. Higher harmonic smart springs actuation.

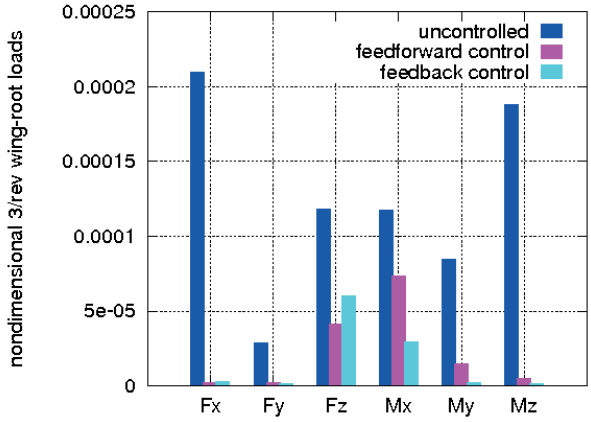

Figure 2. 3/rev wing-root loads. Higher harmonic pitch actuation.

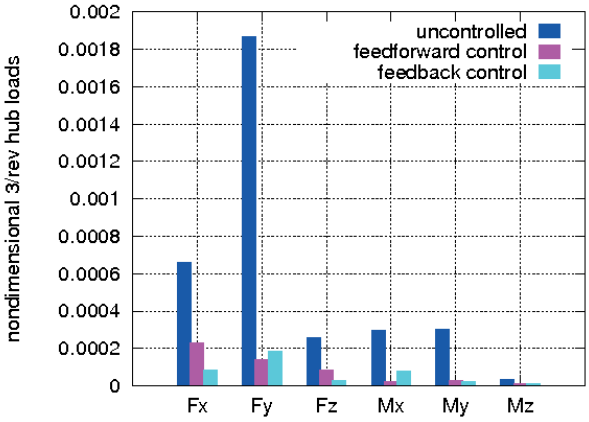

Figure 5. 3/rev proprotor hub loads. Higher harmonic pitch and smart springs actuation.

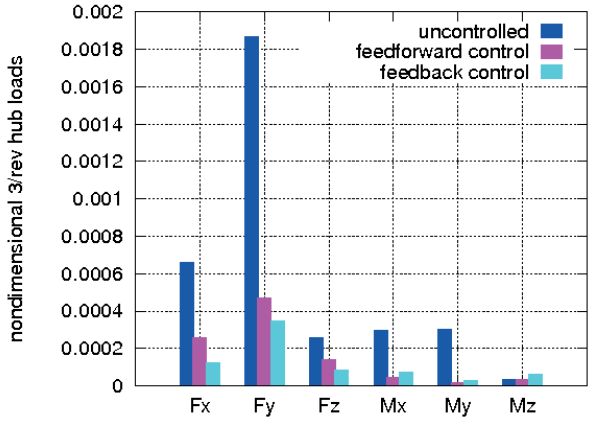

Figure 3. 3/rev proprotor hub loads. Higher harmonic smart springs actuation.

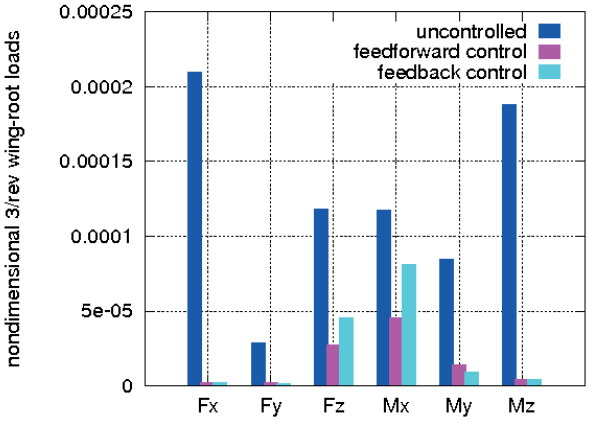

Figure 6. 3/rev wing-root loads. Higher harmonic pitch and smart springs actuation.

[2] Nguyen, K., Betzina, M. and Kitaplioglu, C., "Full-Scale Demonstration of Higher Harmonic Control for Noise and Vibration Reduction on the XV-15 Rotor," *Journal of the American Helicopter Society*, Vol. 46, No. 3, 2001, pp 182-191.

[3] Nitzsche, F., Grewal, A., and Zimcik, D., "Structural Component having Means for Actively Varying its Stiffness to Control Vibra-

tions," U.S. Patent No. 5,973,440, 999. European Patent EP-996570-B1, 2001.

[4] Gennaretti, M., Molica Colella, M., and Bernardini, G., "Analysis of Tiltrotor Airframe Vibratory Loads Transmitted by the Wing-Proprotor System," 9th Int'l Conference on Fluid-Induced Vibration (FIV 2008), Prague, Czech Republic, 2008.

[5] Gennaretti, M., and Bernardini, G., "Novel Boundary Integral Formulation for Blade-Vortex Interaction Aerodynamics of Helicopter Rotors," *AIAA Journal*, Vol. 45, No. 6, 2007, pp. 1169-1176.

[6] Hodges, D.H., and Dowell, E.H., "Nonlinear Equation for the Elastic Bending and Torsion of Twisted nonuniform Rotor Blades," NASA TN D-7818, 1974.

[7] Gennaretti, M., and Bernardini, G., "Aeroelastic Response of Helicopter Rotors Using a 3-D Unsteady Aerodynamic Solver," *The Aeronautical Journal*, Vol. 110, No. 1114, 2006, pp. 793-801.

[8] Hodges, D.H., and Ormiston, R.A., "Stability of Elastic Bending and Torsion of Uniform Cantilever Rotor Blades in Hover with Variable Structural Coupling," NASA TN D-8192, 1976.

[9] Morino, L., "A General Theory of Unsteady Compressible Potential Aerodynamics," NASA CR-2464, 1974.

[10] Patt, D., Liu, L., and Friedmann, P.P., "Rotorcraft Vibration Reduction and Noise Predictions Using a Unified Aeroelastic Response Simulation," *J. of the American Helicopter Society*, Vol. 50, No. 1, 2005, pp 95-106.

[11] Zhang, J., "Active-passive hybrid optimization of rotor blades with trailing edge flaps," Ph.D. Dissertation, Department of Aerospace Engineering, The Pennsylvania State University, 2001.

[12] Anusonti-Inthra, P., and Gandhi, F., "Helicopter vibration reduction through cyclic variations in rotor blade root stiffness," *Journal of Intelligent Material Systems and Structures*, Vol. 11, No. 2, 2000, pp 153-166.

[13] Johnson, W., "Self-tuning regulators for multicyclic control of helicopter vibration," NASA TP-1996, 1982.

[14] Johnson, W., "Dynamics of Tilting Proprotor Aircraft in Cruise Flight," NASA TN D-7677, 1974.

[15] Johnson, W., "Analytical Modeling Requirements for Tilting Proprotor Aircraft Dynamics," NASA TN D-8013, 1975.

[16] Molica Colella, M., "Sviluppo di una Metodologia per l'Analisi Aeroelastica di Configurazioni Ala-Rotore" Tesi di Laurea, Università Roma Tre, 2006. (in Italian)